Chapter 1

Water: A Molecule Endowed with Extraordinary Physicochemical Properties

1.1. Molecular geometry and electrical properties

A water molecule consists of an oxygen atom bonded to two hydrogen atoms. In water, each hydrogen atom is bound to the oxygen by a pair of electrons. However, only two of the six outer-shell electrons of oxygen are used to form covalent bonds, the remaining four being organized into two non-bonding pairs (Figure 1.1). The four electron pairs surrounding the oxygen tend to arrange themselves as far from each other as possible in order to minimize repulsions between these clouds of negative charge. However, the two non-bonding pairs exert a strong repulsion against the two covalent bonding pairs, which results in a deformed tetrahedral geometry with a H–O–H angle of 105° instead of the theoretical angle of 109°. As a result, the H_2O molecule is electrically neutral even though the electrical charges are not distributed uniformly. Indeed, a negative charge is associated with the oxygen atom while the hydrogen atom carries a positive charge (Figure 1.2). This electronic configuration defines the polar structure of water molecules, which consequently have a mutual attraction and tend to stick together.

This process is called "hydrogen bonding" and explains why water is a liquid instead of a gas under standard conditions (close to the Earth's surface pressure and temperature conditions). In comparison to a covalent bond, the hydrogen bond is so weak that the timescale of its life expectancy is in the order of the picosecond (10^{-12} s), therefore explaining the low molecular viscosity of water (10^{-3} N·s·m^{-2} at 20°C) compared to many other liquids at a given temperature. This low molecular viscosity plays a key role in the regulation of osmotic pressure in body fluids.

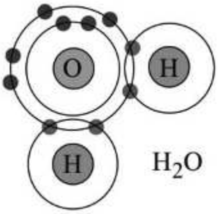

Figure 1.1. *Bonding and non-bonding electronic pairs of the outer shell in the water molecule*

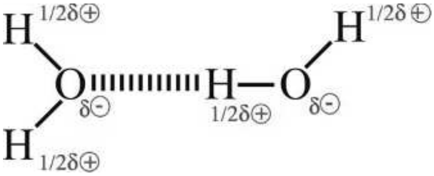

Figure 1.2. *The dipolar water molecules forming hydrogen bonding*

In ordinary ice, each water molecule forms four hydrogen bonds to the nearest oxygen neighbors with O–O distances of 2.76 Å (Figure 1.3). The triple O angles are 109° according to a lattice structure with a tetrahedral coordination. This basic unit is repeated in three dimensions to build the ordinary ice crystals with hexagonal symmetry that can be observed in snowflakes.

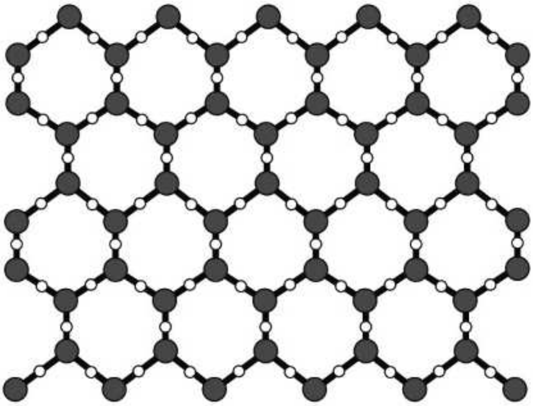

Figure 1.3. *A tetrahedral coordination and hexagonal symmetry of the crystal lattice of water ice*

When ice starts melting and forms a thin layer of liquid water (Figure 1.4), the crystal lattice breaks down as thermal motions distort and finally break hydrogen bonds.

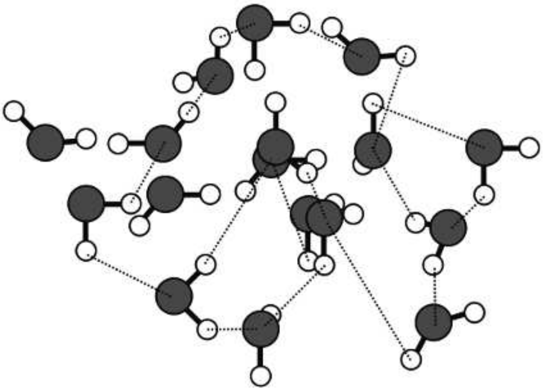

Figure 1.4. *The "disordered" structure of the water molecule*

1.2. Phase diagram

Phase diagrams define fields in temperature and pressure where a substance is characterized by the same chemical composition and physical state. The most popular equation of state was defined for an ideal gas during the second part of the 17th Century and is known as Boyle's law or the Boyle–Mariotte law:

$$\mathrm{PV} = \mathrm{nRT}$$

where P is the pressure, V is the volume, n is the number of moles, T is the absolute temperature and R is the universal gas constant.

In 1873, van der Waals determined the first equation of state able to predict the conditions of coexistence between vapor and liquid phases, which was further refined to give the Redlich–Kwong equation in 1949. More recently, the Helmholtz free energy function (F), applied to a pure substance such as water, was used to determine its thermodynamic properties, such as caloric properties, isochoric and isobaric heat capacity, speed of sound, and differences in enthalpy and internal energy. This work led to the definition of a fundamental equation of state that was proposed by the International Association for the Properties of Water and Steam in 1995 (IAPWS-95) (Figure 1.5).

The Helmholtz free energy function is defined as follows:

$$F = U - TS$$

where U is the internal energy of the system, T is the absolute temperature and S is the entropy. It is noteworthy that F is related to the Gibbs free energy function as follows:

$$G = F + PV$$

In phase diagrams, the physical states of a given substance are defined by fields limited by coexistence curves also called "binodal curves". In pressure–temperature diagrams, the slopes of these curves can be calculated by using the Clausius–Clapeyron equation according to:

$$\frac{dP}{dT} = \frac{\Delta H}{T \Delta V}$$

where ΔH and ΔV are, respectively, the enthalpy and specific volume changes that take place during the phase transition.

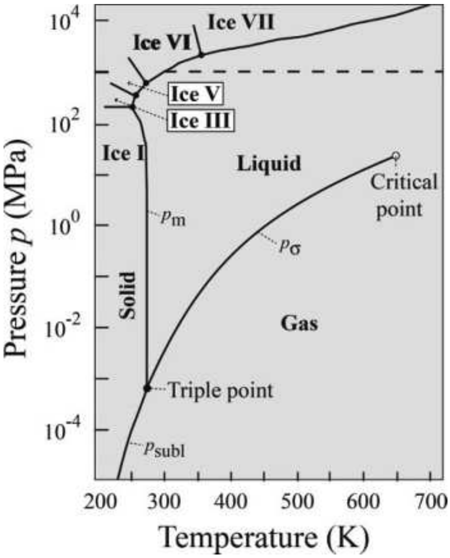

Figure 1.5. *The phase–boundary curves of pure water computed after the equation of state developed according to IAPWS-95 [WAG 02]*

On the Earth, life emerged under *P–T* conditions close to the triple point of water (Figure 1.6), which means that the three phases (gas, liquid and solid) coexist, having identical Gibbs free energies. A “critical point” occurs at the end of a phase line where the properties of the two phases become indistinguishable from each other. Boundary crossings between the solid–liquid–gaseous fields of the phase water diagram correspond to specific processes in the physical state of the H_2O molecule. For example, crossing the boundary from the solid to the gaseous state is called “sublimation”, while the reverse pathway is called “deposition”, the term “condensation” being reserved for the changing state from vapor to liquid water (Figure 1.6).

The known ices, 16 types so far defined, are distinguished on the basis of their structure (Figure 1.7). The low-pressure phases (hexagonal ice (Ih), cubic ice (Ic) and ice (XI)) are characterized by quite a perfect tetrahedral geometry built with the oxygen atoms, while some distortion of the crystal lattice affects the high-pressure polymorphs (ices II–IX and ices XII–XV).

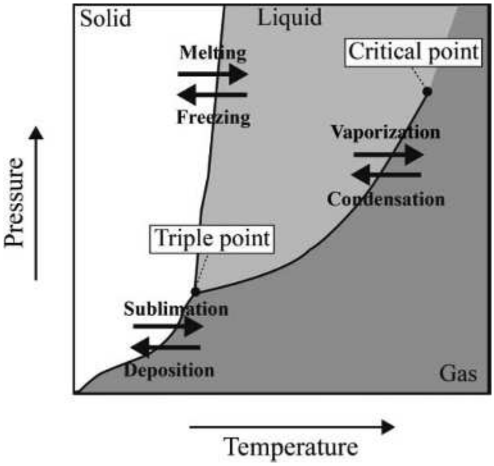

Figure 1.6. *Terms corresponding to phase changes around the triple point of water*

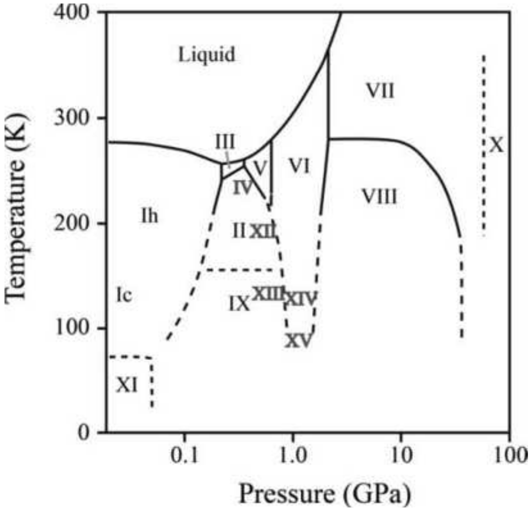

Figure 1.7. *Phase diagram of water with the stability regions for the 16 known polymorphs of ice [COG 11]*

Hexagonal (d = 926 kg·m^{-3}), cubic (d = 933 kg·m^{-3}) ices and ice XI (d = 930 kg·m^{-3}) are less dense than liquid water, whereas the other ices are all denser than liquid water with densities reaching up to 2,785 kg·m^{-3} for ice X (Table 1.1).

Ice structure	d (kg·m^{-3})
Ic	933
Ih	926
II	1,195
III	1,160
IV	1,275
V	1,233
VI	1,314
VII	1,591
VIII	1,885
IX	1,160
X	2,785
XI	930
XII	1,301
XIII	1,247
XIV	1,294
XV	1,328

Table 1.1. *Densities of the 16 known ice polymorphs [COG 11]*

As pressure increases, the ice phases become denser by bending their atomic bonds and interpenetrating their lattices more and more. The existence of ice at high pressure has important implications for the chemical composition, density and rheology of planetary interiors, especially those of large satellites of the giant planets. At pressures and temperatures higher than those defining the critical point in the liquid–vapor space, water is in a supercritical state, which means that it exists as liquid-like hydrogen-bonded clusters dispersed within a gas-like phase where alternating physical properties between gas-like and liquid-like behaviors vary in response to small variations in density. The supercritical water is a strong oxidizer, has low viscosity, dielectric constant and hydrogen bonding; it is also a poor solvent for electrolytes but a powerful solvent for non-polar molecules.

From the phase diagram of water, two intriguing issues can be highlighted. The first issue concerns the boiling temperature of water, which is very high compared to other molecules of similar molar masses (Figure 1.8). Indeed, water with its molar mass of 18.02 g is expected to boil at temperatures far below zero instead of the observed boiling point of 100°C at 1 bar.

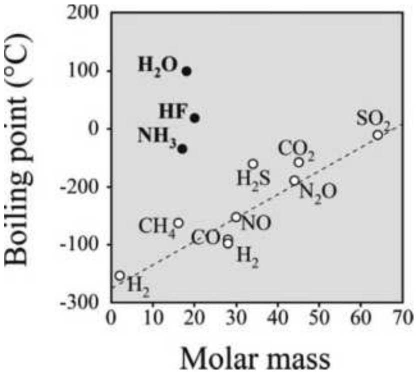

Figure 1.8. *Boiling points of several "light" molecules as a function of their molar mass*

Without H-bonding, water would exist in the world only as a gas, precluding the existence of life on the Earth. An anomalous boiling temperature due to H-bonding is also known for other molecules such as fluorhydric acid (HF) and ammonia (NH_3) (Figure 1.8). As for any other substance, the boiling point of water decreases with decreasing pressure. At high altitudes, the atmospheric pressure is lower than at sea level. For example, water boils at 72°C at the top of the Everest and the cooking of a hard-boiled egg would take twice the time (Figure 1.9).

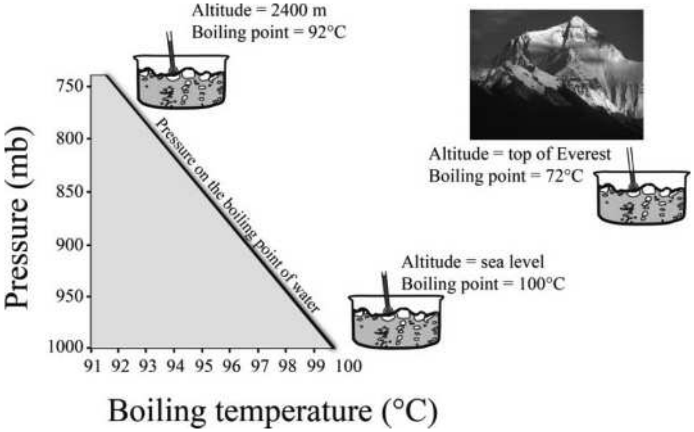

Figure 1.9. *Effect of altitude-dependent atmospheric pressure on the boiling point of water*

The second issue deals with the melting temperature of ice that decreases as pressure increases; in other words, it means that ice melts when pressure increases, which is the consequence of the negative slope of the curve delimiting the fields of ice and water stability (Figure 1.5). The classical point of view is that skaters slide more easily on ice than on any other solids because ice melts under their skate pressure to produce a thin film of water. This is, however, not true because the pressure induced by the blade is not large enough to melt ice at temperatures between –30°C and –3°C, a temperature range compatible with ice skating. Indeed, the optimum temperature for ice skating is –5.5°C, while it is –9°C for playing hockey. The demonstration can be easily made after integration of the Clausius–Clapeyron equation, assuming that both enthalpy and volume changes are constant, i.e. they are independent of temperature and pressure:

$$P_b - P_a = \frac{\Delta H}{\Delta V}\left(\ln T_b - \ln T_a\right)$$

The volume change during ice-melting ($\Delta V_{\text{melting}}$) can be calculated once the molar mass (M) of water (18.02 g) and densities (ρ) of water and ice are known, which are, respectively, 1,000 kg·m^{-3} and 917 kg·m^{-3}. According to the relationship:

$$\rho = \frac{M}{V}$$

where $\Delta V_{\text{melting}} = -1.63 \times 10^{-6}$ m^{-3} and the enthalpy change during ice-melting (ΔH) equals 6.01 kJ·mol^{-1}. The triple point tells us that ice melts at a temperature T_a of 273.15 K and at a pressure P_a = 1 atm or 101,325 Pa. Temperature T_b corresponds to the temperature at which ice melts when submitted to a pressure P_b resulting from the weight of an ice skater spread over the blade surface of one skate. Considering a weight of 70 kg and a blade with a typical surface of 6×10^{-4} m^2:

$$P_b = \frac{M \times g}{S} = \frac{70 \times 9.806}{6 \times 10^{-4}} = 1.14 \times 10^{6}\ \text{N.m}^{-2}\ \text{or}\ P_a$$

where g is the gravitational acceleration constant that equals 9.806 m·s^{-2}.

The decrease of the melting point of ice is only of ≈ –0.1°C at a pressure P_b of 11.4 bars. To decrease the melting point of ice by 5.5°C, which corresponds to the optimum temperature (≈ –5°C) to skate on ice (Figure 1.10), the pressure should correspond to a skater weighing approximately 4,800 kg, close to the average weight of an African elephant.

Figure 1.10. *Ice skaters or how to slide surprisingly on a solid surface*

British scientist Michael Faraday was the first to suspect the phenomenon of “premelting” in the mid-19th Century, or, more precisely, the development of a liquid layer that forms on solids at temperatures below the bulk melting point. X-ray diffraction provides evidence for the existence of a liquid-like layer on the surface of ice whose thickness is of a few dozen nanometers between −25°C and −1°C. Current observations and theoretical modeling suggest that surface-melting is attributable to the interaction of the vibrational motion of the surface molecules with the interior bulk molecules of ice.

1.3. Stable isotopes of hydrogen and oxygen

Hydrogen, the first element in the periodic table, has an atomic mass of 1.007825 with two stable isotopes: ^{1}H or H (protium) and ^{2}H or D (deuterium). Deuterium nucleus contains one proton and one neutron. ^{1}H is the most common hydrogen isotope found in abundance on the Earth, exceeding 99.98%. Protium is a primary product while deuterium was generated by proton–neutron reactions during the Big Bang.

Oxygen has three stable isotopes: ^{16}O (99.76%), ^{17}O (0.04%) and ^{18}O (0.2%). The lighter isotope is the most abundant because it is the most stable nucleus formed in massive stars (mass exceeds that of the Sun eight times), whose core temperatures are higher than 10^{9} K. In these conditions, the light isotope of carbon, ^{12}C, itself issued from a triple-alpha reaction (three ^{4}He nuclei or alpha particles are transformed into one carbon) is able to fuse with ^{4}He to yield ^{16}O. Both ^{17}O and ^{18}O are secondary isotopes produced in subsequent generations of stars. So, ^{17}O results from the burning of hydrogen into helium during the CNO cycle, while most ^{18}O is produced in the helium-rich zones of stars when ^{14}N fuses with a ^{4}He nucleus.

Stable isotope geochemists normalize isotopic ratios to an international reference material, thus allowing inter-laboratory comparisons of isotopic measurements. These normalized isotopic ratios are, therefore, expressed using the so-called δ notation. In the case of oxygen isotopes, two δ notations are used as follows:

$$\delta^{18}O = \left[\frac{{}^{18}O/{}^{16}O_{(sample)}}{{}^{18}O/{}^{16}O_{(SMOW)}} - 1 \right] \times 10^3$$

$$\delta^{17}O = \left[\frac{{}^{17}O/{}^{16}O_{(sample)}}{{}^{17}O/{}^{16}O_{(SMOW)}} - 1 \right] \times 10^3$$

with SMOW (Standard Mean Ocean Water), the international reference or standard; its absolute $^{18}O/^{16}O$ and $^{17}O/^{16}O$ ratios are 2.0052×10^{-3} and 3.76×10^{-4}, respectively. By definition, the $\delta^{18}O$ and $\delta^{17}O$ of SMOW equal 0. This international reference, which was defined by H. Craig in 1961, results from the mixing of several waters sampled in the Atlantic, Pacific and Indian oceans at depths between 500 m and 2,000 m.

In the case of deuterium and hydrogen isotopes, the following δ notation is used:

$$\delta D = \left[\frac{D/H_{(sample)}}{D/H_{(SMOW)}} - 1 \right] \times 10^3$$

where the D/H ratio of SMOW = 1.557×10^{-4}. Any natural or artificial sample enriched in the heavy isotope relative to the SMOW reference has a positive δ value, while any sample with a depletion in the heavy isotope relative to SMOW has a negative δ value. In other words, δ values represent the isotopic ratio of a sample reported in per mil deviations from SMOW.

1.4. Thermodynamic properties

Most specific thermodynamic properties of water are related to its structure and, more specifically, to the existence of hydrogen bonding resulting in an electrical polarization. Water is the only natural molecule that can be observed on Earth in its three states, which are vapor water, liquid water and ice (Figure 1.11). Pressure and temperature conditions at the Earth's surface are such that they are close to the triple point of water. This unique situation for a planetary body in the solar system is largely responsible for the presence of life on Earth.

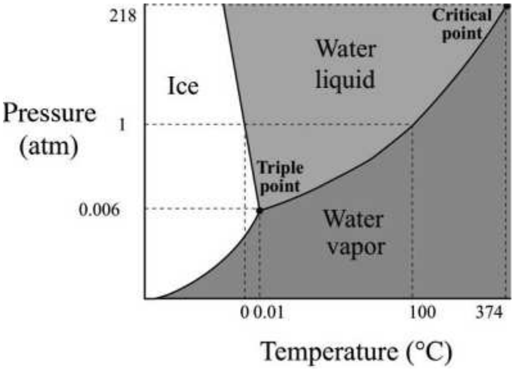

Figure 1.11. *Earth: the only known planet that has P-T conditions close to the triple point of water*

Latent heat is the quantity of heat absorbed or released by a substance undergoing a change of state, such as ice changing to liquid water or liquid water changing to vapor water, at constant temperature and pressure. Water has the highest latent heat of fusion or melting (3.34×10^5 J·kg^{-1}) except NH_3, and one of the highest latent heats of evaporation (2.26×10^5 J·kg^{-1}). The latent heat of water evaporation is the power engine of the water cycle, playing an important role in the transportation of heat toward the poles, thus preventing an accumulation of excess heat in the tropics. As water vapor moves from warm areas to cooler regions, it condenses to form rain, thus releasing heat, which warms the ambient air. The huge amount of energy involved in this cycle generates the winds on the Earth, which, combined with the Coriolis force, ultimately control the global shape of the surface ocean circulation.

Specific heat or heat capacity is the amount of heat necessary to change the unit mass (e.g. a mole) of a substance by one degree in temperature. Water has a very high specific heat of 4.186 × 10^3 J·kg^{-1}·K^{-1}, which is one of the highest of all solids and liquids after NH_3. This means that a lot of energy is needed to increase the temperature of water, another consequence of the energy required to break the hydrogen bonds. As the Earth is covered by 71% of liquid water, solar radiation causes only small changes in the Earth's surface temperature. Heat is stored by the ocean in summer and released back into the atmosphere in winter, reducing the seasonal temperature differences, a remarkable property of the coastal regions located under mid-latitudes.

For most substances, density increases as temperature decreases. However, the density of pure water decreases at temperatures above and below the maximal value of 4°C. This irregular expansion of water is called "anomalous expansion". Ice has a different structure to liquid waters with molecules that self-organize in a regular well-ordered lattice rather than quite randomly as in the liquid phase. From 0°C to 4°C, the vibrational energy of water molecules increases counterbalancing their tendency to form a well-organized 3D structure. Hydrogen bonds become weak or break causing some isolated molecules to fit together more closely, occupying less space, thus resulting in increasing density. Above the threshold value of 4°C, thermal expansion becomes the dominating effect and results in a decreasing density with increasing temperature (Figure 1.12).

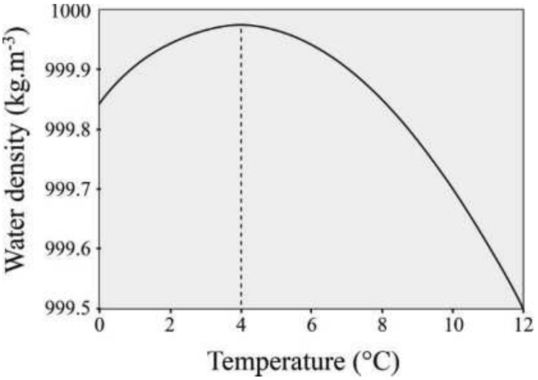

Figure 1.12. *Variations in pure water density as a function of temperature*

An exception is made for “heavy water”, or more precisely deuterium oxide (D_2O), which is water inside which both hydrogen atoms have been replaced by deuterium, the isotope of hydrogen containing one proton and one neutron. Deuterium oxide is indeed denser (1,077 $kg \cdot m^{-3}$ in the standard temperature and pressure conditions) than pure water and its solid phase sinks while it floats in seawater (1,020–1,029 $kg \cdot m^{-3}$). Heavy water is used as a neutron moderator and coolant in nuclear reactors.

The anomalous expansion of water has numerous effects at various spatial and temporal scales on the sea level, deep oceanic circulation and aquatic life. The equation of state of seawater leads to the calculation that an increase in the average ocean temperature by 10°C would raise the sea level by approximately 6 m (Figure 1.13), a scenario that could have taken place during the warmest periods of the Earth’s history, for example, around 90 million years ago during the Cenomanian and Turonian geological periods of the Cretaceous.

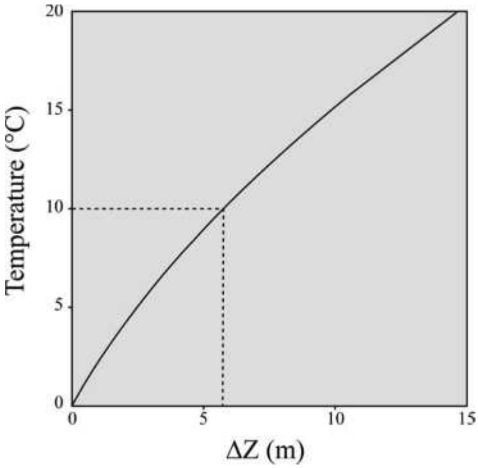

Figure 1.13. *Rising of the seawater level (ΔZ) resulting from the thermal expansion of seawater linked to an increase in the average oceanic temperature*

The knowledge of the equation of state of seawater is fundamental to accurately determine the properties of a seawater mass (see section 3.1). The most common analytical solution for the equation of state of seawater is of polynomial form and is given in [GIL 82]. The solution is presented as a set of equations leading to the calculation of seawater density ρ as a function of temperature T (°C), pressure P (bars) and practical salinity S (see section 3.1). The first step defines the equation for the density ρ_w of pure water ($S = 0$):

$$\begin{aligned}\rho_w &= 999.842594 + 6.793952 \times 10^{-2}\mathrm{T} - 9.09529 \times 10^{-3}\mathrm{T}^2 \\ &\quad + 1.001685 \times 10^{-4}\mathrm{T}^3 - 1.120083 \times 10^{-6}\mathrm{T}^4 + 6.536332 \times 10^{-9}\mathrm{T5}\end{aligned}$$

The second step provides the density of seawater at the atmospheric pressure:

$$\begin{aligned}\rho(\mathrm{S},\mathrm{T},0) = \rho_w &+ \mathrm{S}(0.824493 - 4.0899 \times 10^{-3}\mathrm{T} + 7.6438 \times 10^{-5}\mathrm{T}^2 - 8.2467 \times 10^{-7}\mathrm{T}^3 \\ &+ 5.3875 \times 10^{-9}\mathrm{T}^4) + \mathrm{S}^{3/2}(-5.72466 \times 10^{-3} + 1.0227 \times 10^{-4}\mathrm{T} \\ &- 1.6546 \times 10^{-6}\mathrm{T}^2) + 4.8314 \times 10^{-4}\mathrm{S}^2\end{aligned}$$

The density at pressure P is obtained from the relationship:

$$\rho(\mathrm{S},\mathrm{T},\mathrm{P}) = \rho(\mathrm{S},\mathrm{T},0)/(1 - \mathrm{P}/\mathrm{K}(\mathrm{S},\mathrm{T},\mathrm{P})$$

where K is the secant bulk modulus. For pure water, the bulk modulus is defined as:

$$\begin{aligned}\mathrm{K}_w &= 19652.21 + 148.4206\mathrm{T} - 2.327105\mathrm{T}^2 + 1.360477 \times 10^{-2}\mathrm{T}^3 \\ &\quad - 5.155288 \times 10^{-5}\mathrm{T}^4\end{aligned}$$

As a function of salinity, the relationship becomes:

$$\begin{aligned}\mathrm{K}(\mathrm{S},\mathrm{T},0) = \mathrm{K}_w &+ \mathrm{S}(54.6746 - 0.603459\mathrm{T} + 1.09987 \times 10^{-2}\mathrm{T}^2 - 6.167 \times 10^{-5}\mathrm{T}^3) \\ &+ \mathrm{S}^{3/2}(7.944 \times 10^{-2} + 1.6483 \times 10^{-2}\mathrm{T} - 5.3009 \times 10^{-4}\mathrm{T}^2)\end{aligned}$$

and, finally, as a function of pressure, the solution is:

$$\begin{aligned}\mathrm{K}(\mathrm{S},\mathrm{T},\mathrm{P}) = \mathrm{K}(\mathrm{S},\mathrm{T},0) &+ \mathrm{P}(3.239908 + 1.43713 \times 10^{-3}\mathrm{T} + 1.16092 \times 10^{-4}\mathrm{T}^2 \\ &- 5.77905 \times 10^{-7}\mathrm{T}^3) + \mathrm{PS}(2.2838 \times 10^{-3} - 1.0981 \times 10^{-5}\mathrm{T} \\ &- 1.6078 \times 10^{-6}\mathrm{T}^2) + 1.91075 \times 10^{-4}\mathrm{PS}^{3/2} + \mathrm{P}^2(8.50935 \times 10^{-5} \\ &- 6.12293 \times 10^{-6}\mathrm{T} + 5.2787 \times 10^{-8}\mathrm{T}^2) + \mathrm{P}^2\mathrm{S}(-9.9348 \times 10^{-7} \\ &+ 2.0816 \times 10^{-8}\mathrm{T} + 9.1697 \times 10^{-10}\mathrm{T}^2)\end{aligned}$$

When seawater freezes, ice forms as a solid composed mostly of pure water because salt (Na^+, Cl^-, Mg^{2+}, etc.) incorporation is incompatible with the crystal lattice of ice. At 0°C, the density of water ice is 917 $kg{\cdot}m^{-3}$. It means that less than 9% of an iceberg is on the horizon (Figure 1.14).

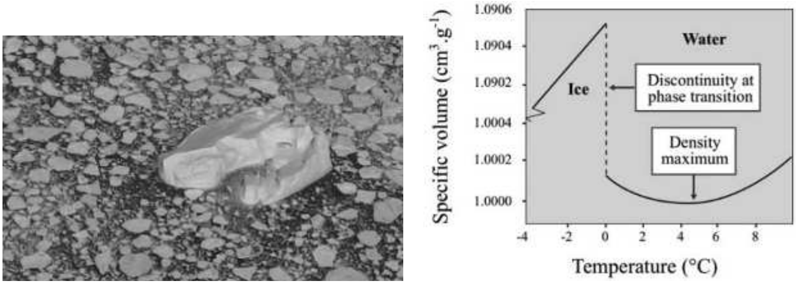

a) **b)**

Figure 1.14. *a) Iceberg (photo: J.-L. Simeon): more than 91% is under the water line; b) density break at the solid–liquid phase boundary of pure water and maximum density value at a temperature of 4°C*

The anomalous thermal expansion of water also plays an important role in aquatic life by only freezing the upper layer of lakes. When the temperature of the surface layer decreases to 4°C, the water body reaches its maximum density and sinks, moving the lower layers of water up, which in turn cools to 4°C and sinks again. When the temperature of the water finally goes below 4°C, the density of water decreases and water no longer sinks. At the end of this convective cycle, surface waters freeze at 0°C whereas bottom waters remain close to 4°C. Only shallow lakes exposed to extremely cold climatic conditions freeze completely. In most cases, the bottom temperature of lakes remains liquid at temperatures close to 4°C. The ice layer floating above forms an insulating barrier to the heat flux flowing into and out from lakes. Dissolved oxygen is trapped beneath the layer of ice and fish and other aquatic animals may continue living in the frozen lakes and ponds (Figure 1.15).

Figure 1.15. *Frozen lakes and underwater life*

The solvent properties of water result from its electrical polarization, which can be measured by the dielectric constant, which represents the ability of a substance to attenuate the transmission of an electrostatic force from one charged body to another. In other words, it also enables a dielectric material to achieve energy storage in a capacitor. The relative dielectric constant is commonly used and is expressed as a value normalized to that of vacuum, considered, by definition, equal to 1. Water has one of the highest relative dielectric constants (80.1 at 20°C) just behind H_2O_2 and HCN. Thus, water is an excellent solvent for charged ions or molecules that are poorly soluble in non-polar organic liquids. As any other substance, increasing the amount of dissolved salt increases the density of the aqueous solution; this explains why the density of seawater is about 1,025 $kg{\cdot}m^{-3}$ on average for an average salinity of 34.5 $g{\cdot}L^{-1}$. Addition of salt also inhibits the formation of hydrogen bonds, which results in the lowering of the freezing point of the aqueous solution (Figure 1.16).

The density of seawater increases with decreasing temperature down to its freezing point that equals −1.9°C for its average salinity of 34.5 $g \cdot L^{-1}$.

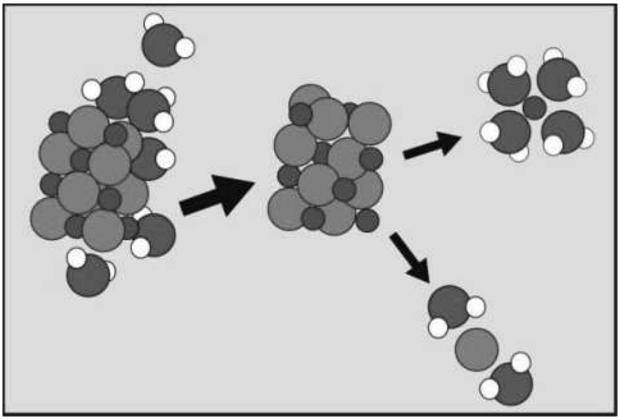

Figure 1.16. *Solvation of a NaCl crystal by H_2O molecules*

The extensive hydrogen bonding in water is responsible for its large cohesion property, which is the mutual attraction between molecules, as well as for its strong adhesion to a solid phase. One consequence of cohesion is that water has one of the highest surface tensions among known liquids with a value of $72.74 \pm 0.36 \times 10^{-2}$ $mN \cdot m^{-1}$ at 20°C, which represents the energy required to increase the surface area of a gas–liquid interface. The strong hydrogen-bonding forces operating among water molecules enables us to distinguish between those located at the air–water interface and those deep inside the bulk liquid. The difference between the forces experienced by these two kinds of water molecules is expressed as the "liquid surface tension". For example, surface tension and adhesion at the evaporative surfaces of leaves induce the forces that trigger water through the vascular system of a plant. Similarly, in animal bodies, water moves through the blood vessels acting as capillary tubes. The surface tension of water also allows some animals of small mass to stay afloat, such as the water strider, *Gerris remigis*, and ant, *Polyrhachis sokolova*, which are both able to move on smooth water surfaces (Figure 1.17).

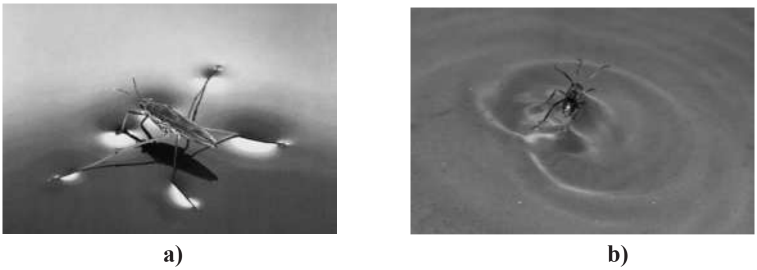

Figure 1.17. *a) The so-called water strider Gerris remigis and b) the semi-aquatic ant Polyrhachis sokolova*

1.4.1. *Conduction of heat*

Heat conduction is the flow of internal energy from a region of higher temperature to a region of lower temperature through the molecular agitation of atoms or molecules without any motion of the material at the bulk scale.

$$\Phi = dQ/dT (\Phi = \text{heat flux and } Q = \text{the amount of heat})$$

Water has the highest heat conduction among all known liquids; it plays an important role in the regulation of body temperature, especially the ability of "warm-blooded" animals to maintain homeothermy (constant body temperature)

1.5. Optical properties

Visible radiation, or light, from the Sun is important for the world's ocean systems for several reasons. It provides the energy necessary for ocean currents and wind-driven waves. Conversion of some of that energy into heat contributes to the formation of the thin layer of warm water near the ocean surface that hosts the majority of marine life. Most significantly, the transmission of light in seawater is essential to the primary productivity of the oceans.

A varying fraction of sunlight is reflected away when it reaches the ocean surface; it is called "albedo". Under similar zenith angles, in windless conditions, the surface of water is smooth and less light will be reflected than under turbulent conditions with many waves increasing the reflecting surfaces. The light that penetrates the surface is refracted because the speed of light is higher in air (2.98×10^8 m·s^{-1}) than in seawater (2.24×10^8 m·s^{-1}). When light is propagated through seawater, its intensity decreases exponentially with depth; this loss in light intensity (W·m^{-2}) is called "attenuation" and results from the combination of two processes: the absorption and scattering of light. Absorption is the process of converting electromagnetic energy into heat or chemical energy; the main seawater absorbers are (1) dissolved inorganic substances, (2) organic and inorganic suspended particles, (3) phytoplankton using available light for photosynthesis, and (4) water itself. Indeed, water appears blue because it preferentially absorbs the long wavelengths of the light spectrum (yellow to red), which can penetrate no more than 50 m, whereas the short wavelengths (green to violet) can penetrate deeper, down to 1,000 m for the clearest seawater during the hours when the sun is the highest in the sky. Below this depth, seawater is permanently dark and the only sources of light are animals with bioluminescent organs (ventral photophores), such as the hatchet fish (*Argyropelecus*). Color and perception of color in the ocean abyss have unexpected and surprising consequences for the adaption of life to these extreme conditions. The ultimate advantage for predators is to see without being seen. Keeping in mind that the only light that travels deep in water is the blue-green light, red and black animals would both appear black, thus invisible to each other, an advantage for prey that should be able to escape predators more easily. Some predators, however, have developed light organs that produce red light while their eyes contain the pigment to detect it. Therefore, a fish like *Pachystomias*, also called "dragonfish", is able to illuminate its preys while remaining visually undetectable (Figure 1.18).

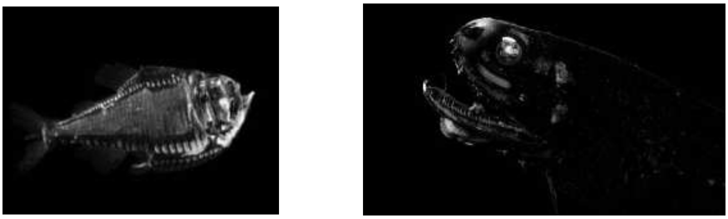

a) **b)**

Figure 1.18. *a) Hatchet fish (Argyropelecus) and b) dragonfish (Pachystomias). For a color version of the figure, see www.iste.co.uk/lecuyer/water.zip*

Light scattering indicates changes in the direction of the electromagnetic waves after multiple reflections of light at the surface of the particles suspended in seawater. Both fresh and saline waters are a mixture of dissolved and particulate matters. Seawater loading in particulate matter is called turbidity (cloudy aspect) and greatly affects its optical properties. The larger the amount of suspended particles, the higher the degree of absorption and scattering by these particles suspended in seawater. These suspended particles tend to absorb the shorter wavelengths, which means that turbid waters appear yellow to brown in color. In such turbid waters, only 2% of incident green light penetrates to 10 m depth, compared to 35% in clear water.

The organic molecules created by this process are an important source of energy for many small organisms that constitute the base of the marine food chain. Life in the oceans is ultimately dependent on the light and the related biochemical process of photosynthesis. Water near the seashore is more turbid due to particles and is, therefore, characterized by a decrease in light transmission, even in shallow waters (Figure 1.19). This is the consequence of the large number of particles carried by rivers, the presence of microorganisms, and the role of waves and tides removing debris deposited on the ocean floor.

Figure 1.19. *Turbid waters in Lake Texoma, Oklahoma, USA (source: Google Earth). For a color version of the figure, see www.iste.co.uk/lecuyer/water.zip*

Clear water and nutrient supply (C, N, S, Ca, Si) are key parameters for the development of marine productivity (Figure 1.20). Visible light wavelengths are captured by chlorophyll-bearing marine plants, which grow according to the following photosynthesis pathway chemical reaction:

$$CO_2 + H_2O \rightarrow CH_2O + O_2$$

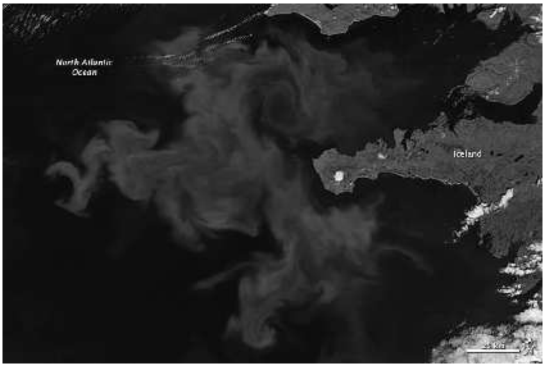

Figure 1.20. *Phytoplankton bloom (grey clouds) located off Iceland (June 24, 2010) (source: NASA). For a color version of the figure, see www.iste.co.uk/lecuyer/water.zip*

The illuminated zone in which light intensity is sufficient for photosynthetic primary productivity to lead to a net growth of phytoplankton is called the photic or euphotic zone. In the clearest waters, i.e. in the central oceanic regions, the photic zone can develop down to depths of 200 m, decreasing to about 40 m over continental shelves, and to as low as 15 m in some turbid coastal waters.

1.5.1. *Turbidity, ternary mixtures and the "Ouzo" effect*

Aniseed-based alcoholic beverages (ABAB) constitute popular refreshing drinks in the warm and sunny countries of the Mediterranean basin. They have distinct proper names depending on the country of origin where they have been manufactured. For example, it is "Anis del Mono" in Spain, "Pastis" in France, "Sambuca" in Italy, "Mastika" in Bulgaria, "Ouzo" in Greece, "Rakı" in Turkey and "Arak" in Lebanon, Palestine, Jordan, Syria and Israel. All these beverages have a common property; they consist of a three-component mixture of ethanol (≈45 vol%), water (55 vol%) and an essential oil called trans-anethol (≈0.1%). It is commonly consumed with the addition of three to five volumes of water to one volume of ABAB. Upon this addition of water, the beverage immediately turns turbid, with a typical cloudy or milky white aspect; the anise-derived oil initially dissolved in the ABAB spontaneously nucleates homogeneously into numerous 1 µm sized droplets. This phenomenon occurs upon mixing large amounts of water with any solution made of oil at low concentration and dissolved into a hydrophilic solvent (ethanol being the alcohol). When bottled, molar ratios between the ethanol, water and oil are selected in such a way that the oil component is soluble within the mixture giving it a transparent appearance. However, when the ABAB is poured into water, the oil is no longer soluble. Despite a low molar fraction, oil droplets are generated through supersaturation at a local scale. These newly formed matter heterogeneities occurring in ABAB have sizes of the same order of magnitude as visible light wavelengths; therefore, light radiation is scattered in all directions making the beverage look turbid.

The essential oil is extracted from anise (*Pimpinella anisum*), star aniseed (*Illicium verum*) or fennel (*Foeniculum vulgare*), and it is commonly called trans-anethol ($C_{10}H_{12}O$), which is basically a phenylpropene aromatic molecule (1–methoxy–4–(1–propenyl) benzene (Figure 1.21).

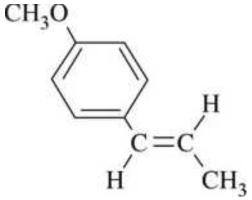

Figure 1.21. *Structural formula of trans-anethol*

In the ternary liquid system defined by water, ethanol and oil (Figure 1.22), a phase diagram is built by reporting the concentration of the solvent on the ordinate as a function of the concentration of the solute on the abscissa, and this at constant temperature and pressure (ambient conditions).

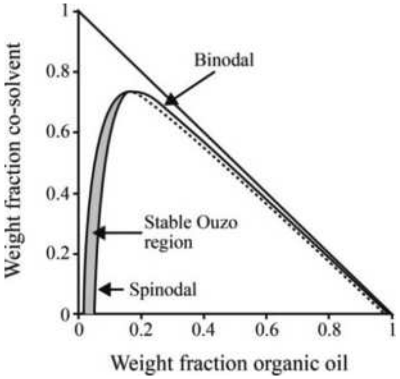

Figure 1.22. *A three-component phase diagram with the location of the metastable turbid "Ouzo-like" beverages between the binodal and spinodal curves [VIT 03]*

For such a phase diagram, the boundary of the unstable region corresponds to the "coexistence" curve, also called "binodal" curve or "miscibility-limit" curve, which is defined by the minimized values of the Gibbs free energy (chemical potentials are equal). Inside the binodal is an area called the "spinodal", which is spatially defined by determining where the curvature of the free-energy curve is negative ($d^2G/dC^2 < 0$), i.e. both binodal and spinodal curves meet at the critical point of the phase diagram. Above the spinodal curve, which illustrates the limit of thermodynamic stability of the system, the process of moving toward equilibrium takes place by homogeneous droplet nucleation that is ultimately controlled by diffusion processes. Between the binodal and the spinodal, any system can survive for quite a long time in a metastable state even though the Gibbs free energy is not fully minimized.

This process of spontaneous and homogeneous nucleation occurring in the unstable region of the ternary phase diagram is also called "spontaneous emulsification"; it must be emphasized here that no mechanical energy such as stirring the solution is required to obtain the homogeneous distribution of 1 μm sized droplets of oil dispersed in the mixture of ethanol and water. The fast polymerization process linked to the "Ouzo effect" is now used to produce nanospheres and nanoparticles, whose size may be smaller in some cases than those obtained by using conventional methods such as evaporation of solvents, ultrasonication or high-shear techniques.

To better understand the Ouzo effect and the thermodynamic properties of the related ternary phase diagram, further investigations can be performed to make the ABAB transparent again to the visible light. One simple experiment can easily be performed at home. Let us prepare a solution at ambient temperature (≈20°C), taking one volume of ABAB diluted with four volumes of water; the resulting solution becomes cloudy white in a time estimated to be in the order of less than 1 ms. Now, add a few drops of transparent liquid soap to the solution and stir gently, it will become transparent in a few seconds (Figure 1.23).

Figure 1.23. *A turbid mixture of one volume of aniseed-based alcoholic beverage mixed with four volumes of water at ambient temperature becomes transparent upon addition of a few drops of liquid soap*

This observation is explained by the physical properties of soap that significantly reduce the size of oil droplets that no longer interfere with the visible light radiations. Indeed, soap, which is chemically the salt of a fatty acid, is on the one hand characterized by a non-polar and hydrophobic (water incompatible) long carbon chain, while, on the other hand, it has a polar ionic ("salt" function) and hydrophilic (water compatible) structure. The soap molecule, acting as a surfactant and a hydrotrope, is therefore able to build bridges between the polar water molecules and the non-polar oil molecules, which form the so-called "micelle" molecular superstructure. As a result, soap is able to efficiently disperse the oil molecules in water, hence these liquids are no longer immiscible.

Miscibility in the liquid ternary phase diagram of ABAB is also obtained without addition of any surfactant substance. For a given composition, miscibility is easily obtained by heating the ABAB. In your kitchen, the aniseed beverage, looking like the milky way, will become transparent once heated on the cooktop at a temperature close to 70°C (Figure 1.24).

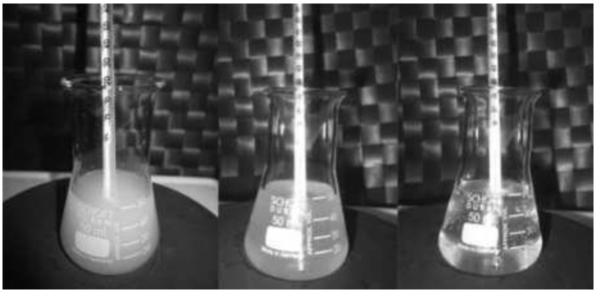

Figure 1.24. *A turbid mixture of one volume of aniseed-based alcoholic beverage mixed with four volumes of water at ambient temperature becomes transparent once heated up to 70°C*

Experiments also reveal that the ultrastructure of ABAB solutions evolve at constant chemical compositions, temperature and pressure because they belong to the metastable region of their related phase diagrams. During the first step, the size of oil particles increases with time according to the so-called process of Ostwald ripening, then the oil separates from the ethanol–water mixture according to the so-called process of "creaming". Ostwald ripening describes a mechanism by which components of the discontinuous phase (here, it is trans-anethol) diffuses from smaller to larger droplets through the continuous phase (here, it is the ethanol–water mixture). Droplet size, hence its stability, increases due to a decrease in Laplace pressure, which also means a decrease in solubility. Ostwald ripening, applied to the liquid–liquid systems, has its equivalent in the liquid–gas system, and it is described by the Kelvin equation:

$$\ln\left(\frac{P}{P_0}\right)=\frac{2\gamma V_m}{rRT}$$

where P_0 is the saturated vapor pressure, γ is the interfacial tension, V_m is the molar volume, r is the radius of the droplet, R is the universal gas constant and T is the temperature.

"Creaming" describes a mechanism of gravity-driven migration of the dispersed component (trans–anethol) within the continuous phase (ethanol–water mixture) due to their differences in density. Under P and T standard conditions, the density of trans-anethol is 988.1 kg·m^{-3}, while that of a 45/55 wt% ethanol–water mixture is only 925 kg·m^{-3}, which means that trans-anethol tends, over time, to sink to the bottom of the glass. This slow evolution towards immiscibility can be observed simply by "forgetting" a glass of any kind of ABAB on your table at room temperature (Figure 1.25).

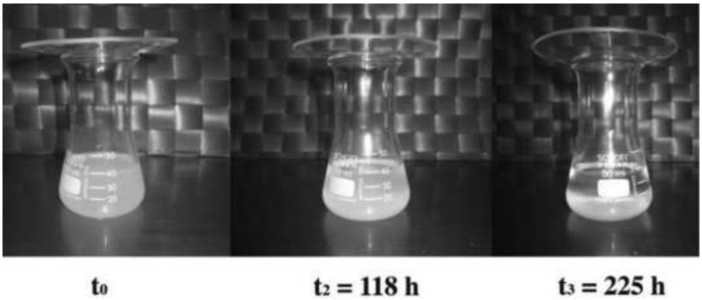

Figure 1.25. *Decreasing turbidity over time of a mixture of aniseed-based alcoholic beverage (one volume for four volumes of water) through combined processes of "Ostwald ripening" and "creaming"*

1.6. Underwater propagation of sound

Sound propagation underwater is important because marine mammals, such as whales and dolphins, or human-made machines, such as boats or submarines, use this physical property either to exchange information or to orient themselves in the ocean. In seawater, the velocity of sound (m·s^{-1}), C, depends on temperature, salinity and pressure, and it is directly related to the depth of the water column according to the following equation:

$$C = 0.016Z + 1.39(S - 35) + 4.6T + 0.055T^2 + 1449.2$$

where Z is the depth in meters, S is the practical salinity and T is the temperature in degree Celsius (°C). As the variations of the salinity S in the ocean remain limited, C variations are mainly controlled by temperature T and pressure P, and are therefore linked to the existence of a thermocline. Indeed, the speed of sound increases with both T and P with typical values of 1,500 and 1,600 $\mathrm{m \cdot s^{-1}}$ in surface waters of salinities equal to 35 $\mathrm{g \cdot L^{-1}}$ and temperature of 10°C and 25°C, respectively. The sound profile with depth exhibits some kind of "hook" pattern with minimum speed values (≈1,480 $\mathrm{m \cdot s^{-1}}$) located approximately 400 m deep; this profile represents oceanic domains where the thermocline is marked all year round, under the tropics, or during the warm season at mid-latitudes (Figure 1.26).

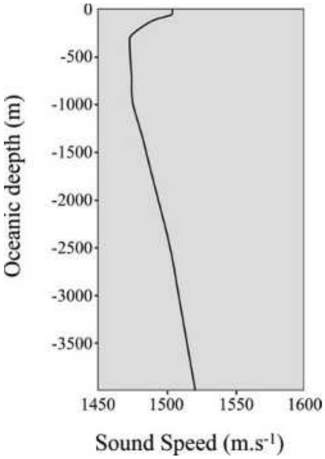

Figure 1.26. *Variations of sound speed as a function of oceanic depth in areas of well-developed thermocline*

As for the refraction of light, sound waves traveling in this low-velocity zone are systematically deflected toward a region of lower velocities. Indeed, waves moving toward the surface are deflected downward while those moving in the direction of deep waters are deflected upward (Figure 1.27). As a result, these sound waves are trapped in a narrow channel usually called Sound Fixing and Ranging (SOFAR) channel, which was discovered in 1943 by a US team led by M. Ewing and J.J. Worzel on the one hand and by the Russian scientist L. Brekhovskikh on the other.

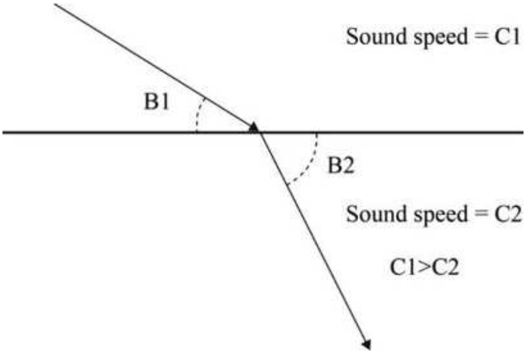

Figure 1.27. *Refraction of sound waves between two water layers of distinct sound speed. The angle of refraction depends on the ratio of sound velocities between the two adjacent water layers*

Sound propagates faster in seawater than in air (≈340 $m \cdot s^{-1}$) but much more slowly than light through seawater; however, sound waves travel much further. Indeed, propagating at a minimum velocity in the SOFAR, sound waves are able to cross long distances over more than 20,000 km, and therefore constitute a kind of natural long-range communication network. Frequencies of interest range from approximately 30 Hz to 1.5 MHz. Sound intensity decreases with distance from the source because of two main processes: the spreading loss and the attenuation resulting from both absorption by water and reactions of chemical dissociation (mainly boric acid and magnesium sulfate), and scattering through reflection by suspended particles such as aeolian dust and organic debris.

1.7. Synthesis and electrolysis

Synthesis of water can be easily achieved by burning 2/3 of H_2 with 1/3 of O_2. This highly exothermic reaction can be accompanied by an explosion. Inversely, the water molecule can break down into H_2 and O_2 gases through an electrochemical reaction driven by an electrical energy, which is called the electrolysis of water. In 1800, Alessandro Volta built the world famous "voltaic pile", followed the same year by William Nicholson and Anthony Carlisle who used this invention for the electrolysis of water. Electrolysis is considered as an ecological way to produce hydrogen gas assuming that the electrical power source is derived from renewable energies. Solar, aeolian, geothermal energies and hydroelectricity can constitute the energy supplies for promoting the electrolysis of water.

Electrolysis of pure water requires excess energy to overcome the activation barriers, which is derived from an electrical power source such as a battery, and which is connected to noble metal electrodes immersed in a bath. Hydrogen is formed at the cathode while oxygen is produced at the anode (Figure 1.28).

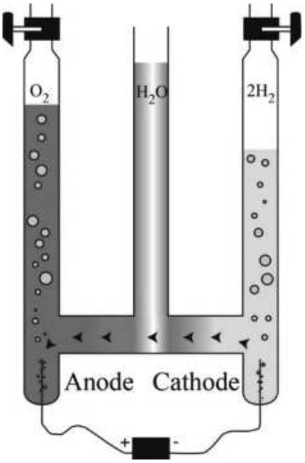

Figure 1.28. *Schematic view of the Hoffman experimental apparatus designed for the electrolysis of water*

The rates at which both O_2 and H_2 are released are related to the current intensity that passes through the electrochemical cell. In pure water, the ionic species, H^+ and OH^-, coexist according to the following equilibrium equation:

$$H_2O \leftrightarrow H^+ + OH^-.$$

A reduction reaction takes place at the cathode:

$$2H^+ + 2e^- \rightarrow H_2$$

An oxidation reaction occurs at the anode:

$$2H_2O \rightarrow O_2 + 4\,H^+ + 4e^-.$$

These half reactions are balanced with those involving the base OH^-:

Cathode: $2H_2O + 2e^- \rightarrow H_2 + 2OH^-$

Anode: $4OH^- \rightarrow O_2 + 2H_2O + 4\,e^-$

In pure water electrolysis, there are no side reactions that could produce by-products; thus, the net balance is obtained by combining half reactions as follows:

$$2H_2O \rightarrow 2H_2 + O_2$$

The minimum necessary cell voltage for the start-up of the electrolysis, E^o_{cell}, is given under standard conditions as follows:

$$E^o_{cell} = -\Delta G_o/nF$$

where n is the number of electrons involved in the reaction, ΔG_o is the variation in the Gibbs free energy under standard conditions and F is the Faraday constant.

1.8. Bibliography

[BRI 35] BRIDGMAN P.W., "The pressure–volume–temperature relations of the liquid, and the phase diagram of heavy water", *Journal of Chemical Physics*, vol. 3, pp. 597–605, 1935.

[COG 11] COGONI M., D'AGUANNO L.N., KULESHOVA N., *et al.*, "A powerful computational crystallography method to study ice polymorphism", *The Journal of Chemical Physics*, vol. 134, pp. 204506–1, 2011.

[CRA 61] CRAIG H., "Standard for reporting concentrations of deuterium and oxygen–18 in natural waters", *Science*, vol. 133, pp. 1833–1834, 1961.

[FOF 83] FOFONOFF N.P., MILLARD R.C., "Algorithms for computation of fundamental properties of seawater", *UNESCO Technical Papers in Marine Science*, vol. 44, pp. 1–53, 1983.

[GAN 05] GANACHAUD F., LATZ J.L., "Nanoparticles and nanocapsules created using the Ouzo effect: spontaneous emulsification as an alternative to ultrasonic and high–shear devices", *ChemPhysChem*, vol. 6, pp. 209–216, 2005.

[GIL 82] GILL A.E., *Atmosphere–Ocean Dynamics*, Academic Press, London, 1982.

[GRI 03] GRILLO I., "Small–angle neutron scattering study of a world–wide known emulsion: Le Pastis", *Colloids and Surfaces: Physiochemical Engineering Aspects*, vol. 225, pp. 153–160, 2003.

[LOB 98] LOBBAN C., FINNEY J.L., KUHS W.F., "The structure of a new phase of ice", *Nature*, vol. 391, pp. 268–270, 1998.

[PER 98] PERROT P., *A to Z of Thermodynamics*, Oxford University Press, p. 329, 1998.

[ROS 05] ROSENBERG R., "Why ice is slippery?" *Physics Today*, vol. 58, pp. 50–55, 2005.

[SCH 08] SCHOLTEN E., VAN DER LINDEN E., THIS H., "The life of an anise–flavored alcoholic beverage: does its stability cloud or confirm theory?", *Langmuir*, vol. 24, pp. 1701–1706, 2008.

[VIT 03] VITALE S.A., KATZ J.L., "Liquid droplet dispersions formed by homogeneous liquid–liquid nucleation: 'The Ouzo Effect'", *Langmuir*, vol. 19, pp. 4105–4110, 2003.

[WAG 02] WAGNER W., PRUSS., "The IAPWS formulation 1995 for the thermodynamic properties of ordinary water substance for general and scientific use", *Journal of Physical and Chemical Reference Data*, vol. 31, pp. 395–478, 2002.

[WAR 99] WARK K., RICHARDS D.E., *Thermodynamics*, 6th ed., McGraw-Hill, Boston, MA, p. 1164, 1999.